Clay Minerals, (2015) **50**, 249–272

Qualitative and quantitative mineralogical composition of the Rupelian Boom Clay in Belgium

E. ZEELMAEKERS[1,2,*], M. HONTY[3], A. DERKOWSKI[4], J. ŚRODOŃ[4], M. DE CRAEN[3], N. VANDENBERGHE[1], R. ADRIAENS[1], K. UFER[5] AND L. WOUTERS[6]

[1] *Laboratory of Applied Geology and Mineralogy, University of Leuven, Celestijnenlaan 200E, 3001 Leuven-Heverlee, Belgium,* [2] *Presently at Shell International Exploration & Production, The Hague, The Netherlands,* [3] *Institute of Environment, Health and Safety, Belgian Nuclear Research Centre (SCK·CEN), Boeretang 200, 2400 Mol, Belgium,* [4] *Institute of Geological Sciences, Polish Academy of Sciences, Research Centre in Kraków, ul. Senacka 1, PL-31002 Kraków, Poland,* [5] *BGR/LBEG, Stilleweg 2, 30655 Hannover, Germany, and* [6] *NIRAS-ONDRAF, Kunstlaan 14, 1210 Brussels, Belgium*

(*Received 17 September 2014; revised 14 June 2015; Associate Editor E. Ferrage*)

ABSTRACT: The Boom Clay Formation of early Oligocene age, which occurs underground in northern Belgium, has been studied intensively for decades as a potential host rock for the disposal of nuclear waste. The goal of the present study is to determine a reference composition for the Boom Clay using both literature methods and methods developed during this work. The study was carried out on 20 samples, representative of the lithological variability of the formation. The bulk-rock composition was obtained by X-ray diffraction using a combined full-pattern summation and single-peak quantification method. Siliciclastics vary from 27 to 72 wt.%, clay minerals with 25–71 wt.% micas, 0–4 wt.% carbonates, 2–4 wt.% accessory minerals (mainly pyrite and anatase) and 0.5–3.5 wt.% organic matter. This bulk-rock composition was validated independently by major-element chemical analysis. The detailed composition of the clay-sized fraction was determined by modelling of the oriented X-ray diffraction patterns, using a larger sigma star (σ^*) value for discrete smectite than for the other clay minerals. The <2 μm clay mineralogy of the Boom Clay is qualitatively homogeneous; it contains 14–25 wt.% illite, 19–39 wt.% smectite, 19–42 wt.% randomly interstratified illite-smectite with about 65% illite layers, 5–12 wt.% kaolinite, 4–17 wt.% randomly interstratified kaolinite-smectite and 2–7 wt.% chloritic minerals (chlorite, "defective" chlorite and interstratified chlorite-smectite). All modelled clay mineral proportions were verified independently using major-element chemistry and cation exchange capacity measurements. Bulk-rock and clay mineral analysis results were combined to obtain the overall detailed quantitative composition of the Boom Clay Formation.

KEYWORDS: Boom Clay, quantitative mineralogy, clay mineralogy, Belgium.

The Boom Clay Formation is a clay-rich Oligocene marine sedimentary deposit in Belgium that has been studied intensively for several reasons: it represents the historical unit stratotype of the Rupelian stage; it has geotechnical properties, often key in civil engineering projects and the clay has been used extensively in coarse ceramics in the past and is still used today. The Boom Clay deposit is now best known for its underground

* E-mail: edwin.zeelmaekers@shell.com
DOI: 10.1180/claymin.2015.050.2.08

laboratory and research site for long-lived intermediate and high-activity nuclear waste disposal in Belgium (ONDRAF/NIRAS, 2013). Therefore, the mineralogy and in particular the quantitative clay mineralogy of the Boom Clay Formation is of great practical importance and has been studied extensively in the past (Thorez, 1976a; Vandenberghe, 1978; Decleer, 1983; Vandenberghe & Thorez, 1985; Bonne, 1989; Goemaere, 1991; Bouchet & Rassineux, 1993; Merceron *et al.*, 1993; Laenen, 1997; Wouters *et al.*, 1999).

The large differences in bulk mineralogy, reported by these studies (Table 1) can be attributed in the first place to sedimentological differences in the silt and carbonate content, which will determine the proportions of quartz, clay minerals, calcite and feldspars (see Vandenberghe *et al.*, 2014).

However, the reported clay fraction compositions vary greatly, not only quantitatively, but also qualitatively (Table 1) and this latter variability is too great to give credibility to the value of these analyses. Most of these results were generated using X-ray diffractometry (XRD) and suffer from: (1) the lack of standardized sample preparations; (2) the use of qualitative methods that were highly descriptive of 00l reflections upon different treatments, but did not take into account the physical nature of the clay phases present, particularly the interstratified minerals (e.g. Thorez, 1976b); and (3) the use of semi-quantitative analysis methods that relied only on the 00l peak height or approximate area measurements.

Thus, the present study was undertaken to address these issues by applying to a representative

TABLE 1. (*Upper*) Quantitative bulk mineralogy of the Boom Clay (wt.%), as reported by: (1) Decleer *et al.* (1983), (2) Merceron *et al.* (1993), (3) Griffault *et al.* (1994), (4) Volckaert *et al.* (1994), (5) Laenen (1997), (6) Wouters *et al.* (1999). (*Lower*) The <2 μm clay mineralogy of the Boom Clay from literature data: (1) Laenen (1997), (2) Decleer (1983), (3) Vandenberghe (1978), (4) Goemaere (1991), (5) Heremans *et al.* (1980), (6) Bouchet & Rassineux (1993), (7) Merceron *et al.* (1993), (8) Thorez (1976a). (modified from Laenen, 1997).

	1	2	3	4	5	6
Clay minerals	56	65	58	60	13–73	30–71
Quartz	24–58	20–25	20	20	16–60	15–53
Plagioclase	3–6	4–5	2.8	3	0.1–10.6	2–5
K–feldspar	6.5–11	4–5	6	5–10	0.7–9.9	1–5
Calcite	0–4.3		1		0–14.6	0–3
Dolomite			0.9	1–5		0
Siderite			0.4	1–5	0–2.8	0–0.3
Pyrite	0.7–2.5	4.5	4.2	1–5	0.7–2.5	0.6–3.5
Rutile/anatase			1			0–1
Organic matter			3.5	1–5		0.5–2

	1 AV. σ *n* = 210		2 AV. σ *n* = 21		3 AV. σ *n* = 18		4 AV. σ *n* = 17		5	6	7	8
Sme	40	8	54 11	15	5	7	3	20	40–50	20–30	20–40	
I/S	9	2	–	12	7	10	3	0	–	–	0–25	
Ilt	19	4	19	5	48	6	25	2	25	23–35	20–30	20–25
Kln	30	6	27	8	20	5	24	2	0	15–25	20–30	–
Chl	3	1	–	6	3	–	0	5–10	–	–		
C/V	–	–	–	15 2	10	–	20–30	–				
Vrm	–	–	–	–	30	–	–	10–25				
I/V	–	–	–	13 3	15	–	–	10–25				

AV. = average; σ = standard deviation; *n* = number of samples studied; Sme = smectite; I/S = randomly interstratified illite-smectite; Ilt = illite; Kln = kaolinite; Chl = chlorite; C/V = randomly interstratified chlorite-vermiculite; Vrm = vermiculite; I/V = randomly interstratified illite-vermiculite.

https://doi.org/10.1180/claymin.2015.050.2.08 Published online by Cambridge University Press

set of Boom Clay samples: (1) internationally accepted and well established standardized sample-preparation methods (Jackson, 1975; Moore & Reynolds, 1997; Środoń *et al.*, 2001); (2) a bulk analysis method with a proven record of highly accurate and repeatable results (e.g. Kleeberg, 2005; Omotoso *et al.*, 2006); (3) modelling of the oriented diffraction patterns of the extracted clay fractions (e.g. Sakharov *et al.*, 1999); and (4) independent verifications of the bulk and clay-fraction results from supplemental major element chemical analyses and cation exchange capacity (CEC) measurements.

The primary purpose of applying the above methods was to determine the qualitative and quantitative bulk and clay-mineral compositions of the Boom Clay. In addition, by applying the independent verification approaches, secondary information on mineral chemical compositions and calculated petrophysical properties were obtained. All these methods were applied to characterize the Boom Clay as a material only, without discussing the geological implications of the analyses further. The relationship between mineralogy and sedimentology has been discussed in a recently published review of the geology of the Boom Clay (Vandenberghe *et al.*, 2014).

THE BOOM CLAY FORMATION AND THE SELECTION OF SAMPLES

The Belgian Boom Clay is a marine sediment deposited during the Lower Oligocene (Rupelian) in the North Sea Basin at 50–100 m depositional depth (Vandenberghe & Mertens, 2013). Shortly after deposition the environment became reducing as is shown by the common occurrence of pyrite in the Boom Clay. At present the clay contains about 20 wt.% of water and the samples analysed were never buried deeper than about 300 m. The outcrop area constitutes the Rupelian historical unit stratotype succession. At the time of deposition, tectonic subsidence affected a large area of northern Europe as a distal reaction to on-going Alpine compression and at the same time water depths varied due to fluctuating global sea-level in response to the build-up of a significant Antarctic cryosphere.

The main lithological properties of the Boom Clay are the rhythmic alternation of silty- with more clay-rich layers of some tens of dm thickness and the occurrence of organic-rich layers of similar thickness and of carbonates, mostly unmixed into horizons with septarian carbonate concretions. Based on these lithological properties the Boom Clay Formation is subdivided into four Members; all layers are numbered and all characteristic septaria horizons have a separate S-number (Fig. 1). Details of the lithostratigraphy of the Boom Clay can be found on the Belgian National Stratigraphic Commission website (http://ncs.naturalsciences.be).

The Boom Clay Formation crops out along the Rupel River and along the Scheldt River south of Antwerp. It dips slightly to the northeast where it is covered by Neogene sediments; the maximal burial depth of the top of the Boom Clay in Belgium – outside the Roer Valley Graben – is slightly more than 300 m and the maximum thickness is almost 150 m (maps in Welkenhuysen *et al.*, 2012). Towards the southwest, the Boom Clay has been eroded and in the outcrop area less than half of the originally deposited clay has been preserved.

The layers in the Boom Clay are highly continuous and laterally and lithologically homogenous (Vandenberghe *et al.*, 2001); therefore the sample selection was focused on the vertical lithological variations within the Boom Clay. Twenty samples representative of the vertical lithological variations known from previous sedimentological studies (Vandenberghe, 1978; Vandenberghe *et al.*, 2001) were collected from the walls of exploitation pits in Sint-Niklaas (Belsele-Waas, Waasland), in Rumst-Terhagen (near Boom, along the Rupel) and in Kruibeke (south of Antwerp along the Scheldt River) and from the core of the ON-Mol-1 well (Fig. 1; Supplement 1). Files containing supplementary information have been deposited with the Principal Editor and are available at www.minersoc.org/pages/e_journals/dep_mat_cm.html. This sample set can be considered representative as the mineralogical variation in the preserved Boom Clay deposits.

METHODOLOGY

Sample preparation

The sample preparation method proposed by Środoń *et al.* (2001) was followed for bulk mineralogical analysis. Air-dried samples were hand-ground to <0.5 mm and milled in methanol for 5 min in a McCrone Micronizing Mill together

https://doi.org/10.1180/claymin.2015.050.2.08 Published online by Cambridge University Press

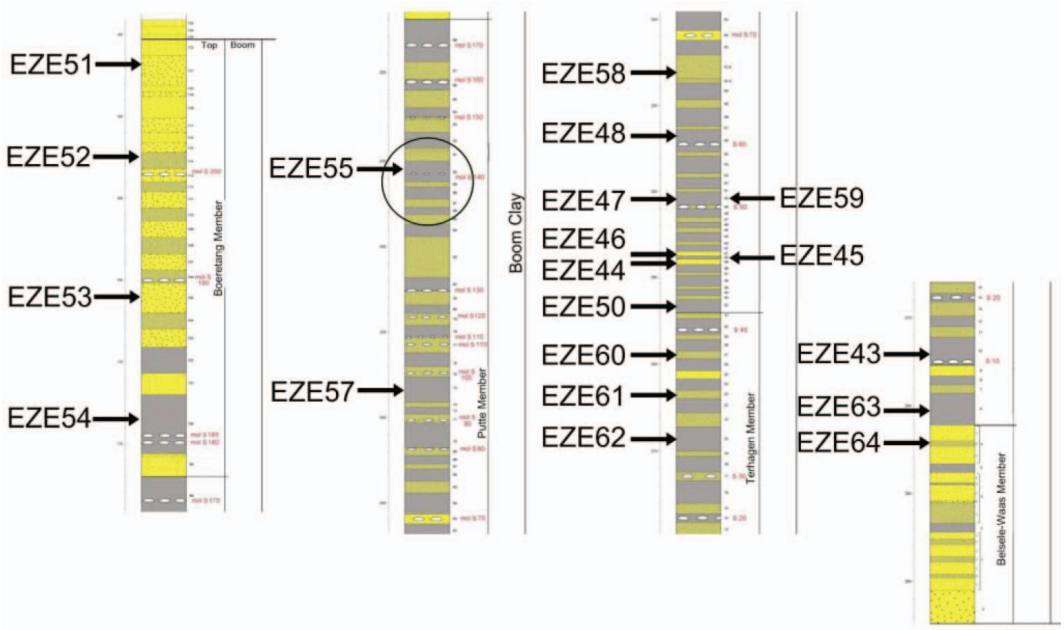

FIG. 1. Core and borehole samples (Table 1) along the detailed lithostratigraphic log of the Boom Clay Formation north Belgium (Vandenberghe *et al.*, 2014). The circle refers to the stratigraphic level of the HADES Underground Research Facilities.

with 10 wt.% of a zincite internal standard. The resultant powder was side-loaded into a specially designed sample holder for XRD analysis.

The hand-ground <0.5 mm material was also used to extract the clay fractions (<2 μm and <0.2 μm). The extraction techniques involve the removal of carbonates, organic matter and Fe-(oxy-) hydroxides followed by grain-size fractionation by centrifugation (Jackson, 1975). The extracted clay fractions were converted to their Ca-form; as expandable layers in this cation state, clay minerals have low susceptibility to ambient humidity variations (Eberl *et al.*, 1987; Sakharov *et al.*, 1999). In addition, cation saturations with Mg and K were prepared for specific identification purposes.

Smear mounts and sedimentation slides were prepared from the <2 μm fractions for pattern-quality comparison purposes. Only small differences on experimental diffraction patterns were observed for clay mineral ratios between these different types of preparation. However, the sedimentation slides produced stronger intensities and less noise because of the better preferred orientation of the clay minerals. Therefore, they were chosen as the preferred oriented-slide-preparation method, for both the <2 μm and <0.2 μm size fractions. Infinite thickness was achieved by depositing 11–12 mg of clay per cm^2 of glass slide (Moore and Reynolds, 1997).

X-ray diffraction analysis

All samples were recorded on a Philips PW1830 X-ray diffractometer with: CuKα radiation, goniometer radius = 173 mm, proportional detector PW3011/00, graphite crystal monochromator, divergence slit 1º, receiving slit 0.1º and soller slit 2.3º, scanning step size of 0.02º2θ, scanning time of 2 s/step and scanning range for powder samples of 5–65º2θ and for oriented slides of 2–47º2θ.

Bulk-rock analysis

For the bulk samples, in a first step the different mineral phases were identified using standard identification procedures as described by Moore and Reynolds (1997). The quantitative composition was determined using the *Quanta* software (Chevron ETC proprietary). In contrast to other full-pattern methods in clay mineralogy such as the Rietveld approach (Ufer *et al.*, 2012), *Quanta* is

https://doi.org/10.1180/claymin.2015.050.2.08 Published online by Cambridge University Press

based on the summation of pre-recorded standards and combines the advantages of both full-pattern summation and single-peak quantification methods. In this method phyllosilicates are quantified based on their 060 reflections and are reported in groups. Both the method and the software have been demonstrated to be highly accurate and repeatable (Kleeberg, 2005; Omotoso *et al.*, 2006).

Clay-fraction analysis

The qualitative and quantitative composition of the clay fractions was determined by modelling the experimental diffraction patterns obtained from oriented slides of the extracted clay fractions using the *Sybilla* software (Chevron ETC proprietary). *Sybilla* combines the formalism for calculating the diffraction patterns of interstratified clay minerals presented by Drits & Sakharov (1976), with a user-friendly graphical interface. During modelling the "multi-specimen" method proposed by Sakharov *et al.* (1999) was used. This method requires that a model should produce satisfactory fits to the experimental patterns in at least two states, glycolated and air-dry. A fit is considered satisfactory if a close match is achieved for peak positions, peak ratios and peak shapes using realistic input parameters for each layer type and proportions of the different layer-types in interstratified minerals. Modelled layer-type parameters include: mean crystal size thickness, *d* spacing, Fe content, K content (illitic layer-types) and water and glycol contents for expandable layer types. Besides satisfactory fits in both glycolated and air-dry states, it is also necessary that these fits produce the same or similar quantitative compositions in both states, while using the same layer-type parameters and proportions. The only exception is the proportion of one and two layers of the saturating fluid (water and ethylene glycol), which are expected to change significantly between the two states due to a larger expression of charge heterogeneity and strong dependence on relative humidity in the air-dry state (e.g. Ferrage *et al.*, 2007). In addition, specific additional treatments have to be applied and combined to identify the different chloritic minerals and to investigate whether vermiculite is present (see the Clay mineral identification section below).

Finally, the sigma star orientation parameter (σ^*) was taken into account. Although Reynolds (1986) suggested that σ^* is set at 12º for all clay minerals during the modelling of oriented diffraction patterns, Dohrmann *et al.* (2009) demonstrated that for unconsolidated and poorly consolidated samples (such as this Boom Clay), the value of σ^* for a discrete smectite is clearly larger than for the other clay minerals. Not taking this effect into account would lead to a significant underestimation of the smectite content. Therefore, in this study the following σ^* values were used in the *Sybilla* software, based on a previous study by Zeelmaekers (2011) on unconsolidated samples: 11º for discrete smectite and 7º for all other phases for the <2 μm fraction and 8º for discrete smectite and 7º for all other phases for the <0.2 μm fraction. Using a trial-and-error approach employing various σ^* ratios, the above values gave a consistent match between the modelled clay content of these samples and independent validations based on major element chemistry and CEC.

CEC measurements

The CEC was determined on bulk samples using the copper(II) triethylenetetramine-method (Amman *et al.*, 2005; Meier & Kahr, 1999; Dohrmann *et al.*, 2012). The standard deviation of the CEC value ($\pm 1\sigma$) was calculated from three independent measurements (three variable weight loads) of the individual sample.

Chemical analysis

Chemical analysis of both major and trace elements was carried out on bulk fractions (<2 μm and <0.2 μm) a commercial service by Activation Laboratories (Ontario, Canada); the quality of the results was monitored by adding the NIST70a and NIST76a reference standards to the sample set: details of the instruments used can be found at www.actlabs.com. Major elements and some trace elements were analysed by a lithium metaborate/tetraborate fusion method; a more extensive set of trace elements was analysed by inductively coupled plasma mass spectrometry (ICP-MS). Boron was determined by using prompt gamma neutron activation analysis (PGNAA), N by thermal conductivity detection after combustion, Cl by instrumental neutron activation analysis (INAA), weight loss at 110ºC ("H_2O^-") and at 1000ºC ("H_2O^+") by gravimetry, FeO by cold acid digestion and titration, C-total/C-graphitic/C-organic/CO_2/S/SO_4 by combustion/infrared

https://doi.org/10.1180/claymin.2015.050.2.08 Published online by Cambridge University Press

detection and coulometry. The factor to convert the C-organic% to the organic matter% (OM%) in a sample (calculated from the H/C and O/C ratios in Boom Clay kerogen (Deniau *et al.*, 2008)) is 1.47, well in line with the conversion factor proposed for more evolved non-soil organic matter (Ignasiak *et al.*, 1985). Additional K_2O analyses, used for the independent checks of the modelling results of the oriented clay fractions, were done on the extracted clay fractions using flame photometry (Sherwood model 420 UK).

Bestrock analysis

The chemical analysis data were used to validate the *Quanta* modelling results by first comparing the actual data with the calculated expected chemical composition from the XRD-derived mineralogical analysis, based on the typical formulae and amounts of the minerals identified in the samples. After an initial agreement between the bulk-rock mineral and chemical compositions has been determined, these two factors can be combined in order to refine the detailed mineral formulae. The *Bestrock* program (Derkowski *et al.*, 2008; Chevron ETC proprietary software), a modification of the *Bestmin* program (see Środoń & Kawiak, 2012; Chevron ETC proprietary software), was used to optimize the bulk-rock analysis results and to calculate the structural formulae of the minerals with a variable chemical composition, using intrinsic relationships and limitations of element contents in each mineral formula. *Bestrock* calculation uses a multi-variable non-linear optimization software package with the *Solver*® engine (Frontline Systems Co., Incline Village, Nevada, USA). In its optimization routine, *Bestrock* is used to combine, statistically, over a set of comparable samples, the elemental chemistry, the CEC and the H_2O adsorbed at 110ºC, together with any other mineralogical information available to help constrain the variable compositions of the minerals. As a second step of the *Bestrock* workflow, the optimized mineral quantities are used to distribute trace elements using linear least-square-based equations with no constraints on element concentrations. Using these results in the final step of the workflow, a set of petrophysical parameters, typically recorded by borehole logging tools, are calculated for the formation studied. The *Bestrock*-calculated petrophysical properties for the Boom Clay were verified by multiple runs with various boundaries and assumptions that returned very similar mineral formulae. Major elements fit the calculated contents with a relative average error of 2%. Trace-element distributions were validated by correlating the measured and calculated bulk-rock values and obtaining R^2 values of 0.97–0.99 with a trend-line slope of 0.988–1.000. The practical value of the *Bestrock* results with respect to wire-log data interpretation and formation evaluation, has been presented in detail by Środoń & Kawiak (2012) and McCarty *et al.* (2015).

BULK ROCK ANALYSIS

Results

The bulk-rock analysis results are reported in Table 2. The wt.% of organic matter (OM), calculated from the C-organic analysis and the wt.% of apatite, calculated from P_2O_5 analysis, were combined with the bulk quantitative results, which were re-normalized to 100 wt.%.

Quartz and the 2:1 clay minerals and micas group (illite, smectite, interstratified illite-smectite, muscovite, glauconite, etc., or "2:1 clays" for brevity) are the dominant minerals. Quartz and "2:1 clays" are inversely correlated because they express the alternation between silty and clay-rich layers. K-feldspar, plagioclase and kaolinite are also present in amounts up to 10–15 wt.%. Samples with the smallest quartz contents also contain minimal amounts of feldspars, confirming that the latter occurs in the very fine sand and coarse silt fractions as was observed previously under the microscope (Vandenberghe, 1978). Calcite is generally absent or present only in amounts of less than 4 wt.%. Dispersed fine carbonate in the Boom Clay is known to occur only in specific stratigraphic intervals or in particular layers that also contain septarian carbonate concretions (Vandenberghe, 1978). That traces (<0.5 wt.%) of siderite and dolomite were detected is in line with the occurrence of very early diagenetic siderite in a few of the septaria levels in the Boom Clay (Laenen & De Craen, 2004) and with geochemical studies that suggested that Boom Clay pore fluids are in near-chemical-equilibrium with siderite, dolomite, calcite and rhodochrosite (Beaucaire *et al.*, 2000). Pyrite is a well-known constituent of the Boom Clay and was detected in all samples; up to 3 wt.%. However, it is difficult to estimate the abundance of pyrite in the entire formation as it occurs

https://doi.org/10.1180/claymin.2015.050.2.08 Published online by Cambridge University Press

TABLE 2. Quantitative bulk-rock results as determined using the *Quanta* software.

Sample	Qz	K-Fel	Pl	Cal	Sd	Dol	Py	Gp	Ant	Ap	OM	ΣNC	Kln	Chl	Σ2:1	ΣC	Tot	CEC
EZE51	46	8	3	0	0	0	1	0	0.5	0.2	0.8	59	3	3	35	41	100	21
EZE52	50	10	4	0	0	0	0.9	0.5	0.5	0.2	0.9	67	3	3	27	33	100	15
EZE53	33	10	4	4	0	0	2	0	0.8	0.2	1.6	56	6	4	35	45	100	16
EZE54	25	7	3	0	0	0	2	0	0.8	0.2	1.3	39	9	3	49	61	100	24
EZE55	32	8	2	4	0	0	2	0	0.6	0.2	1.4	50	8	3	39	50	100	21
EZE57	32	7	3	0.4	0	0	2	0	0.8	0.2	1.3	46	9	3	42	54	100	22
EZE58	43	7	2	0	0.3	0.2	2	0	0.6	0.1	1.5	57	6	3	35	44	100	17
EZE48	22	4	1	0.5	0	0	0.5	0.3	0.8	0.5	1.1	30	12	2	57	71	100	27
EZE59	36	7	2	0.2	0.2	0	3	0	0.6	0.2	2.7	51	8	3	37	48	100	23
EZE47	21	5	1	0	0	0	1	0.5	1	0.2	1.3	31	13	3	54	70	100	25
EZE46	40	6	2	0.5	0	0	1	1	0.5	0.2	1.7	53	7	2	37	46	100	15
EZE45	23	6	2	0	0	0	2	0.7	0.9	0.2	2.9	38	11	4	48	62	100	23
EZE44	61	8	3	0	0	0	0.6	0.5	0.4	0.2	0.9	75	2	2	21	25	100	10
EZE50	25	4	2	2	0	0	3	0.1	0.7	0.2	3.5	40	10	2	47	59	100	24
EZE60	31	8	3	0	0.3	0.4	1	0	0.7	0.2	1.2	45	8	3	43	54	100	22
EZE61	30	8	2	0.1	0.5	0.4	1	0	0.7	0.1	0.7	43	8	3	46	56	100	21
EZE62	23	6	2	0.4	0.3	0.5	3	0.4	0.7	0.2	1.6	37	16	3	44	63	100	20
EZE43	21	5	0.7	4	0	0	2	0	0.7	0.2	0.8	34	10	3	53	66	100	30
EZE63	32	7	2	3	0	1	1	0	0.5	0.1	0.5	47	6	3	44	53	100	22
EZE64	59	7	4	0.1	0	0	2	0	0.4	0.1	0.5	73	4	1	23	28	100	15

Qz = Quartz; K-Fel = K-feldspar; Pl = Plagioclase; Cal = Calcite; Sd = Siderite; Dol = Dolomite; Py = Pyrite; Gp = Gypsum; Ant = Anatase; Ap = Apatite; OM = organic matter; ΣNC = Sum Non-Clays; Kln = Kaolinite; Chl = Chloritic minerals; Σ2:1 = Sum '2:1 Clays'; ΣC = Sum Clays (Kln + Chl + Σ2:1). CEC = cation exchange capacity (meq/100 g). All results are expressed in wt.% (N.B. due to rounding of numbers by *Quanta* some of the totals are ±1%).

heterogeneously from μm-scale framboids, to mm–cm-scale bioturbation traces and up to cm–dm-scale nodules. Traces of gypsum (<0.7 wt.%) are probably alteration products of pyrite. Secondary gypsum occurs in outcrops of the Boom Clay. Moreover, in many cores tiny gypsum crystals develop readily after sampling due to pyrite oxidation. Remarkably, anatase was detected in all samples, even up to 1 wt.% and in the <2 μm and <0.2 μm fractions of several samples. Authigenic anatase is known to participate in the heavy minerals of the Boom Clay (Vandenberghe, 1978). Traces of apatite (<0.5 wt.%) occur in all samples. Apatite in the Boom Clay is known from the transgressive horizon at the base (Vandenberghe, 1978; Vandenberghe *et al.*, 2002); its occurrence throughout the clay deposit is attributed to fish teeth and other fossil carapaces that are common in the clay (e.g. Laenen, 1998).

The shape of the 060 reflection of the '2:1 clays' indicates dioctahedral minerals with variable Fe content. During the *Quanta* analysis the 060 reflections were fitted by a combination of five clay mineral standards, ranging from Al-rich/Fe-poor to Al-poor/Fe-rich end members and intermediates, indicating a mixture of Al-rich and Fe-rich(er) clay phases. Such an assemblage is also consistent with the glauconites and muscovite reported in the coarser fractions of the Boom Clay by earlier studies (Vandenberghe, 1978; Laenen, 1997). The same holds for small amounts of chlorite minerals identified in the bulk rock (see discussion below). Note that the only information retained from the fit is the quantitative sum of the different 2:1 clay mineral species used for the fit, not the clay mineral species themselves. A test with one of the samples showed that using three rather than five clay mineral standards led to almost identical results for the total amounts of '2:1 clays'. However, the 060 reflection range of the full set of samples analysed was modelled consistently using five standards. As an example, in Fig. 2a the 060 reflection zone of sample EZE61 is shown together with the individual model XRD traces of the five clay mineral standards used to fit the recorded sample

https://doi.org/10.1180/claymin.2015.050.2.08 Published online by Cambridge University Press

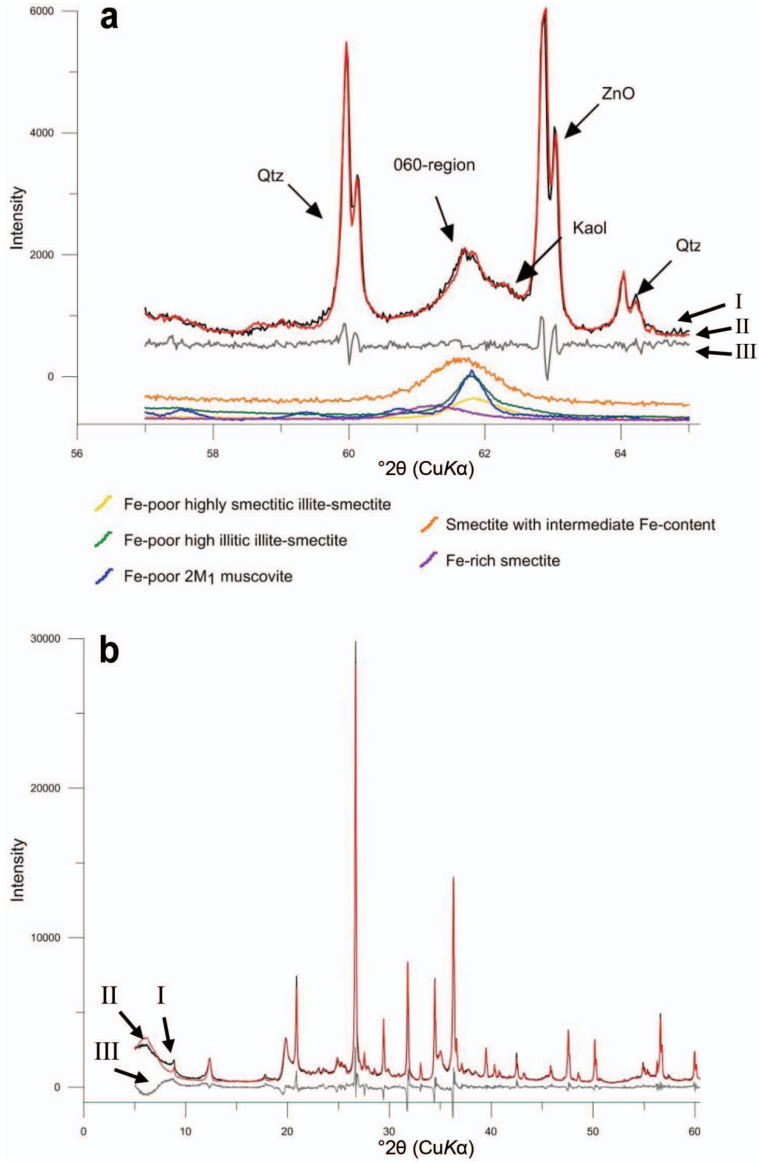

FIG. 2. (a) *Quanta* fit for Boom Clay sample EZE61 concentrating on the 060 region. I – experimental pattern; II – fitted pattern; III – the difference between the experimental and the fitted patterns. The five lower (coloured) patterns are the standards used to fit the 060 region for the '2:1 clays' in the proportions contributing to the total fit. Patterns of the other standards are not shown. (b) *Quanta* fit for Boom Clay sample EZE43, I–III as (a). The quality of fit is representative of the entire sample set.

XRD trace. The intensities of the individual traces are proportional to their contributions in the composite fit. This composite model trace almost overlies the recorded sample trace. The sum of the quantities of the individual standard minerals used is expressed in the bulk composition as 'sum 2:1 clays' minerals (Table 2). In Fig. 2b a comparison is shown over the full 2θ range between a bulk sample diffraction pattern (EZE43) and the pattern summation fit. The similarity between the pattern summation fit and the sample diffraction pattern is exemplary for all samples.

https://doi.org/10.1180/claymin.2015.050.2.08 Published online by Cambridge University Press

Validation of the bulk quantitative results using major-element chemistry

The Boom Clay sample set is suitable for *Bestrock* optimization as the mineralogy is similar for all samples and only the mineral abundances vary. The chemical analyses for the samples studied are shown in Supplement 2.

Based on analyses in the outcrop area in Vandenberghe (1978), Mg and Ca were assumed to be the only exchangeable cations present in the clay minerals; although more recent work on subsurface samples does show Na, Mg, Ca and K in decreasing order of abundance at the exchangeable sites (Griffault *et al*., 1996; Honty, 2010). The variability of exchangeable cations in the Boom Clay is probably a function of carbonate content and different compositions of leaching water in the outcrop zone and in the subsurface. Therefore, in reality there will not be a single exchangeable cation composition for the Boom Clay. The impact of not using Na as an exchangeable cation in the overall calculations proved to be negligible as test runs showed that the optimization process would assign only ~0.03 Na atoms per half unit cell (phuc) to the average structural formula of the '2:1 clays'. The impact of excess Mg assigned to exchangeable cations is equally negligible, as most Mg is assigned to the octahedral sheet of the '2:1 clays' and to chlorite and hence has no impact on the estimation of the (very low) amounts of dolomite. The octahedral composition of the '2:1 clays' was constrained partially by an estimate of the Fe content, obtained from the chemical analysis of the extracted clay fraction (see below).

In the *Bestrock* optimization routine, trace phases such as siderite, dolomite and gypsum may appear as valid results in the computed composition even though these phases were not identified during regular bulk-rock XRD analysis as they could occur in quantities below the detection limits of the XRD/*Quanta* method. Thus, the optimization results for these phases should be considered as less reliable than those from regular bulk-rock analysis; final results are shown in Table 3.

Calculation of the petrophysical properties of the Boom Clay

The *Bestrock* analysis tool was designed to calculate the petrophysical properties of the formation studied, by combining the calculation of the structural formulae of variable composition minerals with a statistical distribution of trace-elements over all the minerals present, for the entire sample set (see Środoń & Kawiak, 2012).

TABLE 3. Quantitative bulk-rock analysis optimized with major-element chemistry using *Bestrock* analysis.

Sample	Qz	K-Fel	Pl	Cal	Sd	Dol	Py	Gp	Ant	Ap	OM	ΣNC	Kln	Chl	Σ2:1	ΣC	Tot
EZE51	44	7	3	0	0.1	0.2	1	0.2	0.7	0.2	0.7	57	3	3	37	43	100
EZE52	50	9	4	0	0.1	0.2	0.9	0.5	0.7	0.2	0.8	66	3	3	28	34	100
EZE53	34	10	3	4	0.1	0.2	2	0.2	0.8	0.2	1.5	56	6	4	34	44	100
EZE54	24	7	3	0	0.1	0.2	2	0.2	0.9	0.2	1.3	39	10	3	48	61	100
EZE55	31	7	2	4	0.1	0.2	2	0.2	0.8	0.2	1.4	49	9	3	40	51	100
EZE57	30	6	3	0.4	0.1	0.2	2	0.2	0.9	0.2	1.2	44	10	3	43	56	100
EZE58	41	7	2	0	0.3	0.2	2	0.2	0.7	0.1	1.4	55	6	3	35	45	100
EZE48	21	4	1	0.5	0.1	0.2	0.5	0.3	0.9	0.5	1	30	13	2	56	70	100
EZE59	36	6	2	0.2	0.1	0.2	3	0.2	0.8	0.2	2.5	51	7	3	39	49	100
EZE47	21	5	1	0	0.1	0.2	1	0.5	0.9	0.2	1.2	31	14	3	52	69	100
EZE46	41	6	2	0.5	0.1	0.2	1	1	0.7	0.2	1.6	55	7	3	35	45	100
EZE45	24	5	2	0	0.1	0.2	2	0.7	0.9	0.2	2.7	38	12	4	47	62	100
EZE44	60	9	3	0	0.1	0.2	0.6	0.5	0.6	0.2	0.8	74	2	2	22	26	100
EZE50	25	4	2	2	0.1	0.2	3	0.1	0.8	0.2	3.3	41	9	2	49	59	100
EZE60	30	9	3	0	0.3	0.4	1	0.2	0.9	0.2	1.1	45	9	3	43	55	100
EZE61	31	9	2	0.1	0.6	0.4	1	0.2	0.9	0.1	0.7	45	9	3	43	55	100
EZE62	22	6	2	0.4	0.3	0.5	3	0.4	0.9	0.2	1.5	38	17	4	42	62	100
EZE43	20	5	0.7	4	0.1	0.2	2	0.2	0.8	0.2	0.8	33	9	3	55	67	100
EZE63	32	8	2	3	0.1	1	1	0.2	0.8	0.2	0.5	48	5	3	43	52	100
EZE64	58	6	4	0.1	0.1	0.2	2	0.2	0.6	0.1	0.5	72	4	1	24	28	100

https://doi.org/10.1180/claymin.2015.050.2.08 Published online by Cambridge University Press

The trace element distribution over the minerals in the Boom Clay and their calculated petrophysical properties are shown in Supplement 3. Note that the results do not imply that these minerals actually contain these trace elements in the reported proportions, they only imply a statistical association, due to the possibility of trace element-rich heavy minerals being deposited together with certain phases. The high probability of trace-element association with phases such as apatite or anatase does not imply that some of the Boom Clay petrophysical parameters are controlled by these minerals, as they are only present in very small amounts (<1%). The availability of these data can improve the interpretations of well logging in the Boom Clay (see e.g. Wouters *et al.*, 1999).

CLAY-MINERAL ANALYSIS

As expected from the similar qualitative bulk mineralogy of the samples, the clay mineralogy of the Boom Clay is qualitatively homogeneous (Fig. 3).

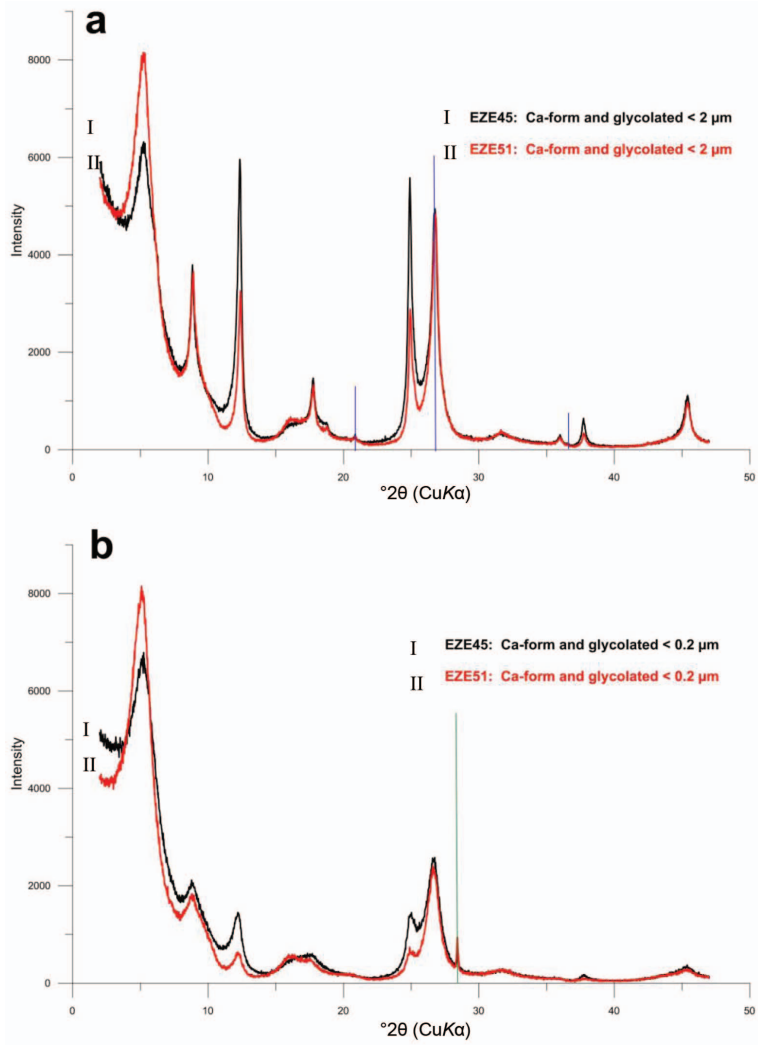

FIG. 3. Diffraction patterns of two glycolated Ca-form Boom Clay samples showing the maximum variability in clay mineralogical composition encountered. (a) <2 µm, the vertical lines identify quartz; (b) <0.2 µm, the vertical line identifies the elemental silicon standard added as a peak position calibration standard.

https://doi.org/10.1180/claymin.2015.050.2.08 Published online by Cambridge University Press

Clay-mineral identification

Illite is identified clearly by its 10 Å and higher-order reflections being almost unaffected by glycolation (Fig. 4). Also, kaolinite is recognized easily from its 7.16 Å and higher-order reflections and their disappearance after heating at 550ºC for 1 h. After glycolation the low-angle tail of the 7.16 Å peak is affected slightly, suggesting an admixture of interstratified kaolinite-smectite. The presence of other expandable minerals is also clearly evident after ethylene glycol solvation. The 17 Å peak suggests smectite and/or randomly interstratified illite-smectite. Diffraction effects upon glycolation are manifested by smeared slopes and plateaus rather than by peaks. Their position between illite and smectite end-member reflections indicates interstratified illite-smectite.

To specify the type of smectite involved, its expandability after Li-saturation and heat treatment of the samples was tested (Greene-Kelly test). Although the Greene-Kelly test is not always very reliable (Moore & Reynolds, 1997), Li-saturation followed by brush-glycerol was applied to the main smectite fractions (<0.2 μm) as this method always confirms the presence of montmorillonite (Vandenberghe & Thorez, 1985).

Chlorite was confirmed by the 13.8 Å reflection after heating at 550ºC for 1 h (Figs 4 and 5). This chlorite 001 diffraction peak is known to be enhanced by the heat treatment while the intensities of higher-order reflections are reduced (e.g. Moore & Reynolds, 1997).

Previous work has shown disagreement over the presence of vermiculite in the Boom Clay, with some authors reporting very low levels and others abundances up to 10–25% (Thorez, 1976a; Heremans *et al.*, 1980). The relatively high CEC of vermiculites could have a significant impact on the sorption properties of the Boom Clay, thus the presence or absence of vermiculite is of great importance when considering the Boom Clay as a potential host formation for the disposal of nuclear waste. For this reason the minor 14.25 Å peak, visible in the XRD pattern of the Ca-saturated glycolated phase (Fig. 5a), was investigated in detail. A layer charge of >0.6 phuc can be used to distinguish vermiculite from smectite. Operationally, however, the distinction is made by saturation with Mg and expanding with glycerol to distinguish vermiculite and chlorite from smectite, followed by saturation with K and heating to 300ºC for 1 h, to distinguish vermiculite from chlorite (Moore & Reynolds, 1997). The diffraction patterns of these tests are shown in Fig. 5. The glycerol was applied directly onto the slide by brush, as higher-charge smectites may not swell fully when exposed to glycerol vapours (B. Sakharov, pers. comm.). Afterwards, a small 14.25 Å shoulder remained and a third order peak of this mineral was visible at 4.73 Å. The non-swelling 14.25 Å peak remaining after Mg-glycerol treatment is not smectite, but it

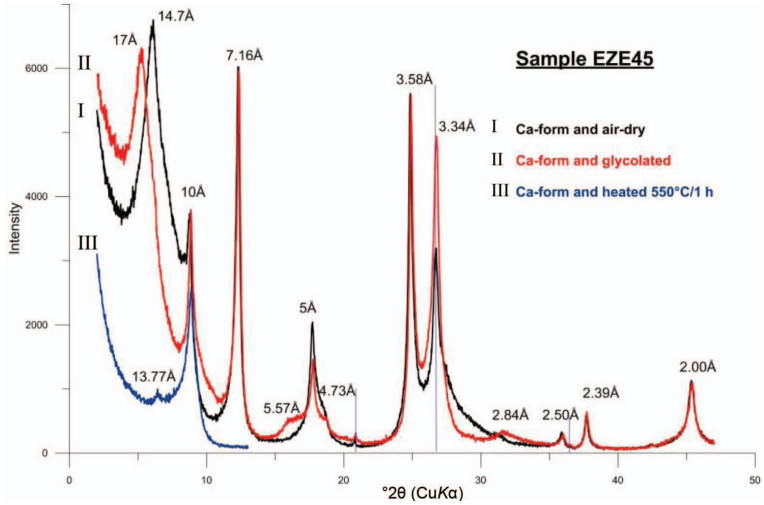

FIG. 4. Diffraction patterns for the: I – air-dry, II – glycolated and III – heated Ca-form <2 μm fraction of sample EZE45; vertical lines indicate quartz.

https://doi.org/10.1180/claymin.2015.050.2.08 Published online by Cambridge University Press

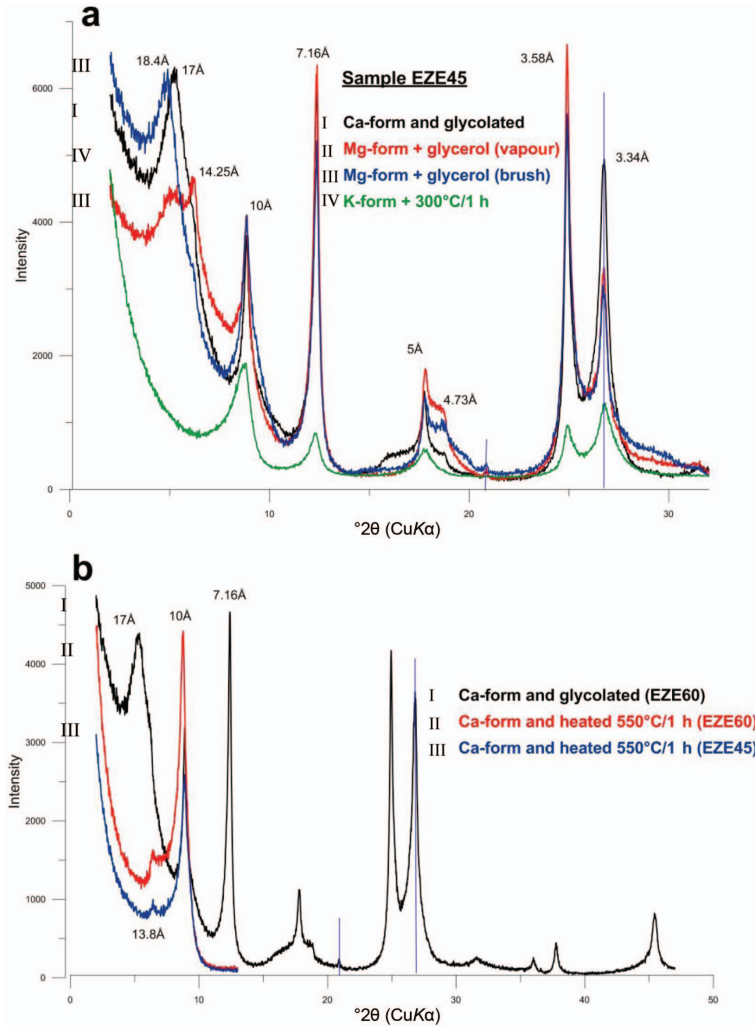

FIG. 5. (a) Oriented diffraction patterns of Ca, Mg and K-saturated samples of the <2 μm fraction of EZE45 showing defective chlorite (14.25 Å/4.73 Å) and a comparison of two glycerol saturation methods. Vertical (blue) lines identify quartz. (b) Comparison of the diffraction patterns of heat-treated (550ºC for 1 h) slides of the Ca-form <2 μm fraction of samples EZE60 and EZE45 showing chlorite-smectite *vs.* discrete chlorite, respectively. Vertical (blue) lines identify quartz.

cannot be vermiculite either as the 001/003 intensity ratio for vermiculite should be much greater than was observed for these samples. This would suggest that this phase should be chlorite. However, upon K-saturation and heating at 300ºC for 1 h, this phase collapses to 10 Å similar to vermiculite, with total disappearance of the 14.25 Å and 4.73 Å peaks (Fig. 5). This behaviour is typical for a defective chlorite in which the interlayer sheet is incomplete, resulting in poor resistance to heat treatment. Such "defective chlorite" has been described as an Fe-rich tri-octahedral mineral (Renngarten *et al.*, 1978; Varentsov *et al.*, 1983; Sakharov *et al.*, 2004).

In addition, the diffraction patterns of the heat-treated (550ºC for 1 h) slides of the Ca-form demonstrate the presence of a randomly interstratified chlorite-smectite phase in some of the samples (e.g. EZE60 in Fig. 5b), based on a diffraction shoulder between the chlorite 13.8 Å reflection and the 10 Å reflection. It is this chlorite-smectite that was described as "degraded" chlorite

https://doi.org/10.1180/claymin.2015.050.2.08 Published online by Cambridge University Press

by Vandenberghe (1978). Figure 5b also shows an example of a sample (EZE45) in which this interstratified phase is absent. The chlorite-smectite phase was identified in several of the outcrop and the core samples, indicating that it is not a recent weathering product, but was already present at the time of deposition (EZE60 shown in Fig. 5b is a core sample). The clay-extraction treatments cannot be responsible for the degradation of the chlorite as the identification of chlorite-smectite ("degraded chlorite") by Vandenberghe (1978) occurred in samples prepared using de-ionized water only.

This detailed investigation of the 14 Å phases in the Boom Clay demonstrates that vermiculite is absent from the Boom Clay and only minor amounts of chlorite, defective chlorite and interstratified chlorite-smectite are present.

Clay-mineral quantification

The oriented slides of the <2 μm fraction of the Boom Clay samples were modelled using the same qualitative approach incorporating six different clay-mineral phases. Four of these were discrete clay minerals: illite, smectite, kaolinite and chlorite; the remainder being randomly interstratified illite- and kaolinite-smectite, both of which were modelled using 3 layer types: illite or kaolinite plus "low charge" or "high charge" smectite layers, in the randomly interstratified structure. In the context of the modelling results described in this section the terms, "low charge" and "high charge", respectively, refer to the presence of two *vs*. one water/glycol layers in the interlayer space. Sometimes the "high charge" component is referred to as "vermiculite layers" (Lindgreen *et al*., 2002; Claret *et al*., 2004). The high *vs*. low charge smectite layers were quantified from the glycolated state model as in the water-saturated state their apparent ratio can vary with relative humidity. For simplicity these interstratified phases are denoted as "illite-smectite" and "kaolinite-smectite".

The results of the clay fraction modelling are gathered in Table 4. Examples of the glycolated and air-dry fits for the same samples are shown in Fig. 6. The discrete illite phase, with a broad 001 reflection and a relatively intense 002 reflection, was best modelled assuming a small amount of smectite layers (1−4%) and no octahedral Fe. Such composition, typical of deep diagenetic and anchizonal illite (Lindgreen *et al*., 2000), is very common in sedimentary rocks sourced, at least partially, from sedimentary terrains. This mineral is further referred to as illite and its abundance ranges from 14 to 25% with an average of 21%. The averages reported in this study refer to the 20 samples examined and do not represent a weighted average for the total Boom Clay volume.

The discrete smectite phase has a modelled Fe content of ~0.5 atoms phuc, which is consistent with earlier studies that used Mössbauer spectroscopy to show that the smectite in the Boom Clay contained octahedral Fe (Decleer, 1983). The ratio of low/high-charge smectite layers in glycolated traces was 89−96/4−11 (Table 4, as percentage layer charge (%LC)). For air-dried smectite these proportions were modelled close to 60:40 (Fig. 6b), indicating charge heterogeneity. The discrete smectite content varies between 19 and 39% with an average of 27%.

The interstratified illite-smectite phase was modelled with a large illite content (64−69%), a small amount of high-charge expandable layers (4−8%) and Fe content of 0.2 atoms phuc. Following the multi-specimen method, the approximate amount of illite in this phase should be preserved when adjusting the model to air-dry conditions and this is indeed observed (68% *vs*. 66% illite layers, Fig. 6a,b). Due to charge heterogeneity, under air-dry conditions the ratio of low/high-charge smectite layers is shifted towards the latter (from 27/5 to 17/17, Fig. 6a,b). The illite-smectite content varies between 19 and 42% with an average of 28%. Figure 6 displays the modelled individual phases illite, smectite and illite-smectite *vs*. the experimental and modelled patterns of a representative Boom Clay sample.

In the kaolinite model only its mean crystal size was adjusted. However, as discussed above, the low-angle tail of its 001 reflection and the high-angle side of its 002 reflection (features G and H on Fig. 6c) indicate the additional presence of a kaolinite-smectite phase. This phase was also modelled using low- and high-charge smectite layer types. However, due to the very small overall contribution of these expandable layers to the samples it is not possible to determine with certainty their exact swelling character. The total expandable content in the kaolinite-smectite was 17−19%. The kaolinite content varies between 5 and 12% with an average of 8% and the kaolinite-smectite content varies between 4 and 17% with an average of 11%.

The distinction between the very small quantities of chlorite, defective chlorite and randomly

https://doi.org/10.1180/claymin.2015.050.2.08 Published online by Cambridge University Press

TABLE 4. Quantitative mineralogy of the <2 μm clay fraction based on the glycolated model.

Sample	— Smectite —		—— Illite-smectite ——			Illite	Kaolinite	Kaolinite-smectite		Chloritic	Total
	%LC	wt.%	%S	det. comp.	wt.%	wt.%	wt.%	%kln	wt.%	wt.%	wt.%
EZE51	96	38	31	69:27:04	26	24	5	81	4	3	100
EZE52	92	33	35	65:29:06	27	23	7	81	7	3	100
EZE53	93	26	32	68:27:05	31	21	7	82	10	5	100
EZE54	89	25	32	68:27:05	30	21	7	82	12	5	100
EZE55	89	25	32	68:26:06	31	22	7	82	11	4	100
EZE58	93	28	32	68:25:07	27	22	9	82	9	5	100
EZE48	93	21	34	66:28:06	27	22	11	82	15	4	100
EZE59	90	24	31	69:23:08	27	22	11	82	10	6	100
EZE47	93	24	33	67:27:06	30	17	9	82	16	4	100
EZE46	93	22	32	68:26:06	28	24	10	82	11	5	100
EZE45	93	23	32	68:27:05	25	25	11	82	11	5	100
EZE44	93	26	31	69:26:05	42	14	5	82	10	3	100
EZE50	93	28	34	66:27:07	34	16	6	82	13	3	100
EZE60	93	19	31	69:24:07	28	25	11	81	10	7	100
EZE61	93	25	32	68:24:08	29	22	8	82	11	5	100
EZE62	93	25	32	68:26:06	19	22	12	82	17	5	100
EZE43	94	37	35	65:29:06	30	15	6	81	10	2	100
EZE63	91	27	31	69:23:08	31	25	7	82	7	3	100
EZE64	93	39	36	64:30:06	26	16	6	83	9	4	100
Average		27			28	21	8		11	4	

%LC = % low-charge smectite layers in smectite; %S = % smectite layers in illite-smectite; det. comp. = detailed composition of the randomly interstratified illite-smectite phase as: *%illite layers:%low-charge smectite layers:%high-charge smectite layers*; %kln = % of kaolinite layers in kaolinite-smectite. The averages refer specifically to the sample set and are not a weighted average for the total Boom Clay volume. Sample EZE57 was not analysed.

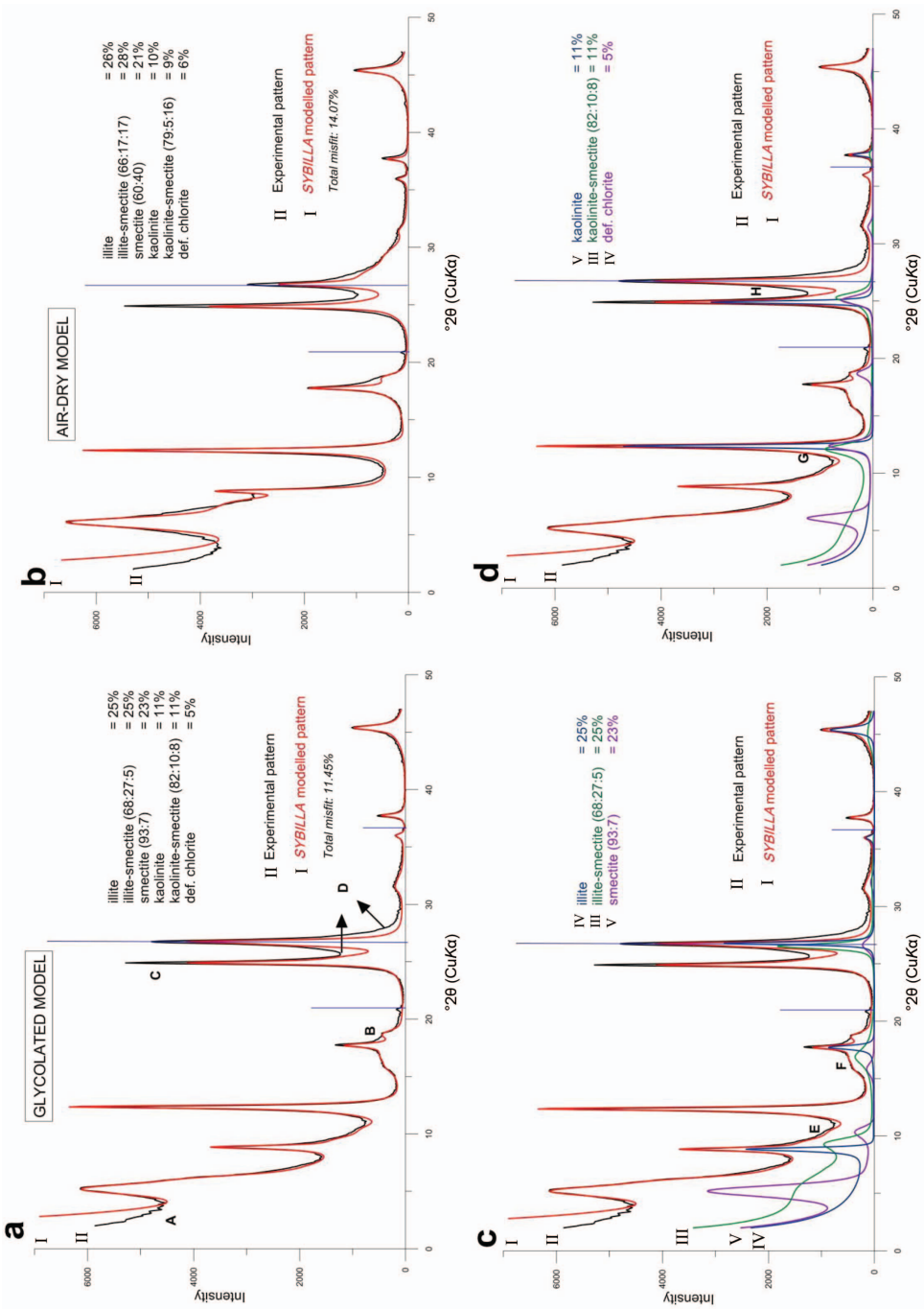

FIG. 6. XRD patterns for Ca-form (<2 μm) EZE45: (a) Glycolated, (b) Air-dry, (c) Comparison of modelled illite, illite-smectite and smectite phases to the glycolated sample (d) Comparison of modelled kaolinite, kaolinite-smectite and defective chlorite phases to the glycolated. I – *SYBILLA* modelled (red); II – Experimental (black); features: A–H discussed in the text. Vertical (blue) lines identify quartz peaks. All results in wt.%.

https://doi.org/10.1180/claymin.2015.050.2.08 Published online by Cambridge University Press

interstratified chlorite-smectite is beyond the resolution of the modelling method. Therefore only one combined 'chloritic' model was used to model the diffraction effects (Table 4). This average model corresponds to a defective chlorite, as a reasonable fit could only be achieved with a partially complete (70%) interlayer octahedral sheet. This structure was modelled with 1 Fe atom phuc in the octahedral sheet and 1.5 Fe atoms phuc in the interlayer octahedral sheet and its abundance in the sample set varies between 2 and 7% with an average of 4%.

Using the same model in similar proportions, the fit of the glycolated and the air-dry models to the experimental patterns is highly satisfactory (Fig. 6a,b). Some areas of mis-fit still exist: the ultra-low angle mis-fit (3–3.5°2θ; Feature A in Fig. 6a) is background only and at the time of the development of the software no mathematical description of the diffraction effects in this region was available (B. Sakharov, pers. comm.). The mis-fit features B and D in Fig. 6a are attributed to natural heterogeneity in the minerals that could not be taken into account sufficiently in the calculated phases. The mis-fit located on the 002 reflection of kaolinite indicated by feature C in Fig. 6c is systematic, but at present unexplained. The mis-fit for the air-dried samples is somewhat larger than for the glycolated samples, as the expandable layer thickness after glycolation is more uniform than after air drying.

The modelling results are supported by the fact that, essentially, a single clay-mineral assemblage model could be used to model the entire sample set satisfactorily. The same set of minerals gave a satisfactory fit to the glycolated diffraction patterns of the <0.2 μm fraction (Fig. 7) after making suitable slight adjustments to certain values, such as: decreasing the mean crystal thicknesses for all phases in this fraction and increasing the expandability of the illite-smectite phase (34% *vs*. 32%) and its high-charge smectite content (14% *vs*. 7%).

Determining the '2:1 clay' mineral formula from elemental analysis of the <0.2 μm fraction

The <0.2 μm fractions of the Boom Clay are not mono-mineralic as demonstrated above, but dominated by the '2:1 clays'. Therefore, it is possible to propose an approximate average '2:1 clay' mineral structural formula.

The chemical analyses of the <0.2 μm are shown in Supplement 4. The P and Mn oxides are not commonly associated with clay mineral lattices and Ti oxide is usually associated with anatase rather than with clay minerals. Chlorite-type minerals are absent from the <0.2 μm fraction. The kaolinite and kaolinite-smectite content obtained from the modelling of the oriented diffraction patterns was used to calculate the amount of SiO_2 and Al_2O_3 to be subtracted from the chemical analysis results to

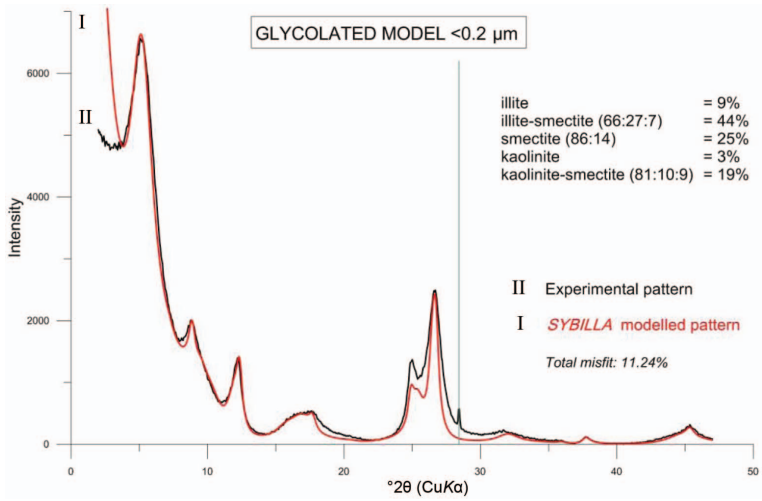

FIG. 7. Glycolated experimental pattern and model for Ca-form <0.2 μm Boom Clay sample EZE45. All results in wt.%. The vertical green line identifies the elemental silicon peak position calibration standard.

https://doi.org/10.1180/claymin.2015.050.2.08 Published online by Cambridge University Press

correct for their presence in the samples. The remaining major-element oxides were used to calculate the structural formulae of the combined '2:1 clays' (illite + smectite + illite-smectite) (Table 5), following the structural formula calculation outlined by Moore & Reynolds (1997). Varying the kaolinite content by a few % did not change the calculated 2:1 clay mineral structural formula substantially. The average structural formula calculated is: $K_{0.33}Na_{0.02}Ca_{0.15}(Si_{3.69}Al_{0.31})(Al_{1.14}Mg_{0.38}Fe_{0.49})O_{10}(OH)_2$.

Independent validation of the clay mineral quantitative results for the <2 μm fraction

The reliability of the quantity of illitic components modelled in the clay fraction, i.e. the discrete illite phase and illite layers from the interstratified illite-smectite, can be evaluated from the K_2O content of this fraction. This is indeed possible because these illitic layers are the only potassium-bearing mineral phases present, as was verified by the random powder recordings of this size fraction. The independent validation was done by comparing the measured K_2O content of the <2 μm fraction to the K_2O content calculated using the *Sybilla* software for the corresponding model. The software makes this calculation by taking into account the modelled illite content in discrete and interstratified minerals, the modelled number of K atoms in each illitic layer type and the modelled crystal size distribution for each K-bearing mineral. The measured K_2O content of the <2 μm fraction (Supplement 5) needed correction as chemical analyses were reported on an air-dry basis, which varies due to the room temperature and relative humidity during the analysis, as opposed to the K_2O content calculated for models in *Sybilla*, which refer to an absolutely dry state. The correction was based on the mass loss of the sample equilibrated at 47% relative humidity under ambient conditions after heating in a thermobalance to 200ºC, which is considered a close approximation of the absolutely dry state (Środoń & McCarty, 2008). The calculated and the analytically measured K_2O contents (after correction) for the <2 μm of all samples are compared Supplement 6. The relative differences are generally <10%. The modelled parameters for the illitic layers and the illite content estimation in the illite-smectite can all be varied somewhat while still producing good diffraction-pattern fits; tests showed that this range of variability leads to relative variations in calculated K_2O content of ~10%. Therefore differences of 10% or less between calculated and measured values are considered a close agreement and an independent validation of the modelling results. This is further supported when considering the very narrow range of the actual K_2O content in the sample set (3.2 to 4.0 wt.%) compared to the absolute possible range of 0 wt.% (a sample containing no illite or illite-smectite) to 11 wt.% (a sample containing only illite).

The total smectitic content was verified independently from CEC measurements. Analogous to the validation of the illitic content a validation was sought for the total smectitic content, being the sum of the discrete smectite phase and the smectite layers from the interstratified illite-smectite. This is based on the assumption that the CEC will be controlled effectively by the smectitic surfaces of these phases and to a much lesser extent by other clay mineral surfaces. The contribution of the expandable layers in kaolinite-smectite was ignored as it only represents a very small fraction of the total clay content.

Due to the relatively large amounts of material required (0.5 to 1 g), CEC measurements could only be performed for the bulk-rock samples. Therefore, the smectitic contents obtained from modelling of the <2 μm fraction were recalculated to give the smectite wt.% contribution to the bulk rock sample. This was done by first splitting the interstratified illite-smectite content into illite and smectite equivalent wt.% based on their modelled proportions. These proportions were added to the wt.% of discrete illite and smectite, respectively, allowing establishment of a smectitic *vs*. illitic content ratio. Finally, this ratio was used to split up the '2:1 clays' content from the bulk analysis into smectitic and illitic content in the bulk rock. This procedure assumes that the ratios between '2:1 clays' in the bulk rock and those in the <2 μm fraction are comparable, which is considered reasonable in the absence of large amounts of coarse-grained micas.

The CEC for an average charged smectite is close to 100 meq/100 g. For example the experimental results in Środoń & McCarty (2008) show an average smectite CEC of 103–110 meq/100 g. Therefore, the CEC value can be considered as an approximation of the smectitic content of the sample and be compared to the smectitic content calculated from the clay-fraction modelling results, as explained above (Table 6, Fig. 8). Table 6 also

https://doi.org/10.1180/claymin.2015.050.2.08 Published online by Cambridge University Press

TABLE 5. Average structural formulae of the '2:1 clays', calculated for the <0.2 μm fractions.

Sample	Si	^{IV}Al	TC	^{VI}Al	Mg	Fe	O.Cat	OC	K	Na	Ca	LC	Kln Corr. (wt.%)	MW
EZE51	3.707	0.293	−0.293	1.228	0.386	0.411	2.025	−0.311	0.282	0.019	0.152	−0.604	6	389.0
EZE52	3.699	0.301	−0.301	1.165	0.403	0.461	2.028	−0.319	0.303	0.017	0.150	−0.620	11	391.2
EZE53	3.675	0.325	−0.325	1.140	0.416	0.471	2.027	−0.334	0.339	0.021	0.150	−0.660	17	392.9
EZE54	3.667	0.333	−0.333	1.156	0.392	0.473	2.021	−0.328	0.340	0.022	0.149	−0.661	19	392.9
EZE55	3.666	0.334	−0.334	1.165	0.391	0.465	2.020	−0.330	0.337	0.023	0.152	−0.664	18	392.7
EZE57	3.667	0.333	−0.333	1.144	0.404	0.488	2.036	−0.296	0.333	0.022	0.138	−0.629	19	392.9
EZE58	3.676	0.324	−0.324	1.124	0.371	0.528	2.022	−0.303	0.312	0.021	0.147	−0.628	18	393.4
EZE48	3.682	0.318	−0.318	1.115	0.358	0.524	1.997	−0.369	0.337	0.015	0.167	−0.686	25	394.2
EZE59	3.680	0.320	−0.320	1.118	0.377	0.523	2.018	−0.323	0.342	0.021	0.140	−0.643	23	394.0
EZE47	3.670	0.330	−0.330	1.120	0.359	0.521	2.000	−0.359	0.333	0.013	0.171	−0.688	24	394.2
EZE46	3.673	0.327	−0.327	1.123	0.370	0.528	2.020	−0.310	0.345	0.013	0.139	−0.637	21	394.1
EZE45	3.674	0.326	−0.326	1.135	0.376	0.501	2.012	−0.339	0.360	0.013	0.146	−0.665	22	394.0
EZE44	3.670	0.330	−0.330	1.148	0.361	0.511	2.020	−0.302	0.360	0.014	0.129	−0.632	18	393.8
EZE50	3.700	0.300	−0.300	1.160	0.369	0.468	1.998	−0.376	0.314	0.019	0.172	−0.675	21	392.0
EZE60	3.681	0.319	−0.319	1.107	0.408	0.509	2.024	−0.335	0.362	0.017	0.138	−0.654	21	394.3
EZE61	3.693	0.307	−0.307	1.116	0.402	0.507	2.025	−0.328	0.337	0.020	0.139	−0.635	20	393.4
EZE62	3.715	0.285	−0.285	1.142	0.402	0.463	2.007	−0.381	0.339	0.020	0.153	−0.666	26	392.3
EZE43	3.703	0.297	−0.297	1.147	0.341	0.513	2.001	−0.337	0.317	0.011	0.153	−0.634	15	392.7
EZE63	3.695	0.305	−0.305	1.125	0.395	0.506	2.026	−0.317	0.359	0.018	0.123	−0.622	11	393.6
EZE64	3.732	0.268	−0.268	1.155	0.381	0.485	2.021	−0.318	0.262	0.014	0.155	−0.586	14	390.3
Average	3.686	0.314	−0.314	1.142	0.383	0.493	2.017	−0.331	0.331	0.018	0.148	−0.644	18	392.9
St. dev.	0.018	0.018	0.018	0.027	0.020	0.030	0.011	0.024	0.026	0.004	0.013	0.027	5	1.4

The original chemistry was corrected for the Kln and Kln-Sme content from modelling of the oriented slides (Table 4) to give Kln Corr. in wt.%.. MW = the molecular weight phuc for each structural formula. (^{IV}Al = tetrahedral Al; ^{VI}Al = octahedral Al; TC = tetrahedral charge; O.Cat = number of octahedral cations; OC = octahedral charge; LC = total layer charge).

TABLE 6. Comparison of the smectitic content and the CEC measured for the bulk rock.

Sample	Bulk-rock smectite content (wt.%)	Bulk-rock CEC (meq/100 g)	Smectitic content as 0.91*CEC (after Środoń, 2009)
EZE51	18	21	19
EZE52	14	15	14
EZE53	16	16	15
EZE54	22	24	22
EZE55	18	21	19
EZE58	17	17	15
EZE48	25	27	25
EZE59	16	23	21
EZE47	26	25	23
EZE46	16	15	14
EZE45	20	23	21
EZE44	10	10	9
EZE50	24	24	22
EZE60	17	22	20
EZE61	21	21	19
EZE62	21	20	18
EZE43	31	30	27
EZE63	19	22	20
EZE64	14	15	14

The bulk-rock smectitic content was calculated proportionately from the wt.% '2:1 clays', determined by modelling, from the bulk-rock analysis (Table 2) of the <2 μm fraction (Table 4). The smectitic content was estimated as 0.91*CEC, assuming a constant charge of 0.41 phuc for smectites (Środoń, 2009).

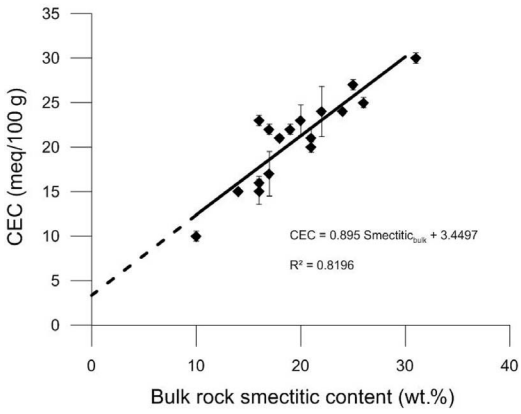

FIG. 8. Measured bulk-rock CEC (in meq/100 g) plotted *vs*. the bulk rock smectitic content, which was calculated by splitting the wt.% '2:1 clays' from bulk-rock analysis (Table 3) according to the proportions determined by modelling of the 2 μm fraction (Table 7). Vertical bars indicate the ±1σ standard deviation.

shows an alternative method of calculating the smectitic content in the bulk rock directly from the CEC using the relationship: smectitic content = 0.91 × CEC (Środoń, 2009), which is based on the assumption of a constant charge of 0.41 phuc for the smectite.

The agreement is close for all three methods, except for two samples (EZE 59 & 60) in which the CEC appears too high compared to the smectitic content. No evident explanation was found for these two exceptions. The linear fit equation shows that between 3 and 4 meq/100 g of the CEC are unexplained by smectitic minerals. This 'supplementary' CEC is assumed to come from illitic surfaces/edges, the smectite layers in the kaolinite-smectite and perhaps the small amounts of organic matter present in the samples.

The kaolinite and chlorite contents were also verified independently by applying the bulk-analysis quantification method described above on the <2 μm fraction. It has been well established that the bulk analysis method used is highly accurate (Kleeberg, 2005; Omotoso *et al.*, 2006); however, 2–3 g of the <2 μm sample would be necessary for

https://doi.org/10.1180/claymin.2015.050.2.08 Published online by Cambridge University Press

this analysis and this was unavailable for most of the samples in this set. Therefore, the validation test was performed on five additional samples of Boom Clay taken over a short interval in the exploitation pit at Rumst-Terhagen in the type area along the Rupel River. To preserve the concept of an independent validation, the exact same detailed model as discussed above was used to model the <2 μm fraction of these samples. The kaolinite and chlorite content obtained was then compared to the values determined by applying the bulk-rock method on the same fraction. Supplements 7 and 8 show that the values for both methods are in good agreement. This agreement is increased even further when the kaolinite-smectite phase is corrected for its smectite content using the expandability determined by modelling (last column, Supplement 7). This correction is necessary as the bulk-analysis method is based on the 060 reflection area where kaolinite and smectite are quantified separately. For both kaolinite and chlorite the independent validations show absolute differences <3 wt.%.

Integration of the bulk-rock and clay-fraction analyses results

As a final step, results from both bulk-rock analysis and the modelling of the extracted clay fraction were integrated by splitting the bulk-rock number for the '2:1 clays' into proportions of illite, smectite and interstratified illite-smectite according to their relative proportions in the <2 μm fraction extracted (Table 7). Further mineralogical specification can be added by detailing the kaolinitic content as consisting of discrete kaolinite and interstratified kaolinite-smectite with ~17−19% expandable layers and detailing the chloritic content as a mixture of chlorite, defective chlorite and a randomly interstratified chlorite-smectite.

This integration of the data again assumes that the quantitative proportions in the clay minerals in the >2 μm fraction are the same as or very close to those in the <2 μm fraction. This assumption is expected to overestimate the smectitic components and underestimate the illitic components slightly due to the smaller grain size of smectitic minerals compared to illitic. In these coarser size fractions, minerals like glauconite and muscovite, identified in microscopy work (Vandenberghe, 1978), will add to the underestimation of the illitic components in our analysis, thus in the current study, muscovite and glauconite were included in the 'illite' fraction. In the same microscopy study some chlorite flakes were also identified in the coarser fraction. The observed quantities of each of these coarser minerals were small in comparison to the overall clay content of the rocks and therefore their impact on the proportions determined will be small.

It is clear from the results presented that, qualitatively, the different Boom Clay samples contain the same minerals in variable proportions. These variations can be understood easily in terms of the lithology types observed in the formation, which are the result of its sedimentological history; while at the same time the provenance of the minerals remains approximately constant during the entire depositional history. The main variations controlled sedimentologically are the proportions of quartz and clay minerals and the contents of carbonates and organic matter.

CONCLUSIONS

The applied methodology, both for the bulk-rock and the extracted clay-fraction analysis, relies on consistent sample pre-treatments and proven quantitative analysis methods. It has permitted a reliable and robust total qualitative and quantitative mineral composition determination for the Boom Clay. All quantitative results were validated independently by chemical and CEC analyses. In addition, cation saturations followed by swelling and heating treatments were used to solve a long-standing discussion regarding the exact nature of the 14 Å components present in the Boom Clay.

The results presented contrast with several previous clay-mineral studies of the Boom Clay which all reported different clay minerals, in widely varying quantities, using non-standardized methods. Such non-standardized approaches led to poor quality diffraction patterns and uncontrolled cation saturation states, thereby impacting severely on reproducibility. Accuracy was also poor because clay-mineral quantification was based solely on a comparison of 001 intensities with standard minerals and the use of correction parameters that were too general. The use in this study of a higher σ^* for smectite than for the other phases in these kinds of poorly consolidated samples is considered a critical factor in being able to determine accurate quantitative proportions successfully from modelling.

Considering the marked improvement in applied methodology, the results of the study presented can

https://doi.org/10.1180/claymin.2015.050.2.08 Published online by Cambridge University Press

TABLE 7. Integration of quantitative bulk-rock data (Table 2) and quantitative clay fraction data (Table 4) by splitting up the 2:1 clays of the former by the proportions determined in the latter.

Sample	Qz	K-Fel	Pl	Cal	Sd	Dol	Py	Gp	Ant	Ap	OM	Kln	Chl	Sme	Ilt-Sme	Ilt	Total	CEC
EZE 51	46	8	3	0	0	0	1	0	0.5	0.2	0.8	3	3	15	10	9	100	21
EZE 52	50	10	4	0	0	0	0.9	0.5	0.5	0.2	0.9	3	3	11	9	7	100	15
EZE 53	33	10	4	4	0	0	2	0	0.8	0.2	1.6	6	4	12	14	10	100	16
EZE 54	25	7	3	0	0	0	2	0	0.8	0.2	1.3	9	3	16	19	14	100	24
EZE 55	32	8	2	4	0	0	2	0	0.6	0.2	1.4	8	3	13	16	11	100	21
EZE 57	32	7	3	0.4	0	0	2	0	0.8	0.2	1.3	9	3					
EZE 58	43	7	2	0	0.3	0.2	2	0	0.6	0.1	1.5	6	3	13	12	10	100	17
EZE 48	22	4	1	0.5	0	0	0.5	0.3	0.8	0.5	1.1	12	2	17	22	18	100	27
EZE 59	36	7	2	0.2	0.2	0	3	0	0.6	0.2	2.7	8	3	12	14	11	100	23
EZE 47	21	5	1	0	0	0	1	0.5	1	0.2	1.3	13	3	18	23	13	100	25
EZE 46	40	6	2	0.5	0	0	1	1	0.5	0.2	1.7	7	2	11	14	12	100	15
EZE 45	23	6	2	0	0	0	2	0.7	0.9	0.2	2.9	11	4	15	16	16	100	23
EZE 44	61	8	3	0	0	0	0.6	0.5	0.4	0.2	0.9	2	2	7	11	4	100	10
EZE 50	25	4	2	2	0	0	3	0.1	0.7	0.2	3.5	10	2	17	21	10	100	24
EZE 60	31	8	3	0	0.3	0.4	1	0	0.7	0.2	1.2	8	3	11	17	15	100	22
EZE 61	30	8	2	0.1	0.5	0.4	1	0	0.7	0.1	0.7	8	3	15	17	13	100	21
EZE 62	23	6	2	0.4	0.3	0.5	3	0.4	0.7	0.2	1.6	16	3	17	13	15	100	20
EZE 43	21	5	0.7	4	0	0	2	0	0.7	0.2	0.8	10	3	24	20	10	100	30
EZE 63	32	7	2	3	0	1	1	0	0.5	0.1	0.5	6	3	14	16	13	100	22
EZE 64	59	7	4	0.1	0	0	2	0	0.4	0.1	0.5	4	1	11	7	5	100	15

Qz = Quartz; K-Fel = K-feldspar; Pl = Plagioclase; Cal = Calcite; Sd = Siderite; Dol = Dolomite; Py = Pyrite; Gp = Gypsum; Ant = Anatase; Ap = Apatite; OM = organic matter; ΣNC = Sum Non-Clays; Kln = Kaolinite; Chl = Chloritic minerals; Sme = Smectite; Ilt-Sme = interstratified illite-smectite; Ilt = Illite. CEC = cation exchange capacity (meq/100 g). All results are expressed in wt.%.

become the reference for the mineralogical composition of the Boom Clay in different application fields.

ACKNOWLEDGMENTS

This study is, in part, the result of a doctoral thesis by EZ at the University of Leuven, Belgium, financed by IWT Flanders and supervised by NV and JŚ. Chevron ETC, Houston is thanked for permission to use the proprietary software *Quanta*, *Sybilla* and *Bestrock*. Victor Drits and Boris Sakharov are thanked for help with the analysis of the exact nature of the 14 Å components. Dorota Bakowska is acknowledged for performing the K_2O analyses. This work was performed in close cooperation with and with the financial support of NIRAS-ONDRAF, the Belgian Agency for Radioactive Waste and Fissile Materials, as part of their program on geological disposal of high-activity and long-lived radioactive waste. The reviewers and editor are thanked sincerely for their constructive comments, which led to considerable improvements of the manuscript.

REFERENCES

Ammann L., Bergaya F. & Lagaly G. (2005) Determination of the cation exchange capacity of clays with copper complexes revisited. *Clay Minerals*, **40**, 441–453.

Beaucaire C., Pitsch H., Toulhoat P., Motellier S. & Louvat D. (2000) Regional fluid charcterisation and modelling of water-rock equilibria in the Boom clay Formation and in the Rupelian aquifer at Mol, Belgium. *Applied Chemistry*, **15**, 667–686.

Bonne A. (1989) *De Mineralogische samenstelling van de Boomse klei*. Report SCK·CEN, NCS89/46/D6265/GV/MVG/N–83.

Bouchet A. & Rassineux F. (1993) *Archimède – Argile. Etude morphologique et minéralogique de trois échantillon d'argile provenant du site de Mol (Belgique)*. Rapport BRGM-ANDRA no. 696–RP–BRG–93–003.

Claret F., Sakharov B.A., Drits V.A., Velde B., Meunier A., Griffault L. & Lanson, B. (2004) Clay minerals in the Meuse-Haute Marne underground laboratory (France): possible influence of organic matter on clay mineral evolution. *Clays and Clay Minerals*, **52**, 515–535.

Decleer J. (1983) *Studie van de relaties tussen chemische, fysische en mineralogische kenmerken van de Boomse Klei en van de verhittingsprodukten*. PhD thesis, University of Leuven (in Dutch).

Deniau I., Devol-Brown I., Derenne S., Behar F. & Largeau C. (2008) Comparison of the bulk geochemical features and thermal reactivity of kerogens from Mol (Boom Clay), Bure (Callovo-Oxfordian argillite) and Tournemire (Toarcianshales) underground research laboratories. *Science of the Total Environment*, **389**, 475–485.

Derkowski A., McCarty D.K., Środoń J. & Eberl D.D. (2008) BestRock - mineralogy, chemistry and mineral surface property optimization to calculate petrophysical properties of the mineral matrix. *Mineralogia – Special Papers*, **33**, 53.

Dohrmann R., Rüping K.B., Kleber M., Ufer K. & Jahn R. (2009) Variation of preferred orientation in oriented clay mounts as a result of sample preparation and composition. *Clays and Clay Minerals*, **57**, 686–694.

Dohrmann R., Genske D., Karnland O., Kaufhold S., Kiviranta L., Olsson S., Plötze M., Sandén T., Sellin P., Svensson D. & Valter M. (2012). Interlaboratory CEC and exchangeable cation study of bentonite buffer materials: I. Cu(II)-triethylenetetramine method. *Clays and Clay Minerals*, **60**, 162–175.

Drits V.A. & Sakharov B.A. (1976) *X-ray Structural Analysis of Mixed-Layer Minerals*. Nauka, Moscow. (in Russian).

Eberl D.D., Środoń J., Lee M., Nadeau P.H. & Northrop H.R. (1987) Sericite from the Silverton caldera, Colorado: Correlation among structure, composition, origin and particle thickness. *American Mineralogist*, **72**, 914–934.

Ferrage E., Lanson B., Sakharov B.A., Geoffroy N., Jacquot E. & Drits V.A. (2007) Investigation of dioctahedral smectite hydration properties by modelling of X-ray diffraction profiles: Influence of layer charge and charge location. *American Mineralogist*, **92**, 1731–1743.

Goemaere E. (1991) *Révision critique de l'analyse par diffraction des rayons X de matériaux at mineraux argileux: Applications à quelques problèmes géologiques et pédologiques à intérêt géotechique; Fascicule III: L' Argile de Boom, Le schistes bitumeneux du Toarcien*. PhD thesis, Université de Liège, Belgique.

Griffault L, Merceron T., Mossmann J. R., Neerdael B., De Cannière P., Beaucaire C., Daumas S., Bianchi A. & Christen R. (1996) Acquisition et régulation de la chimie des eaux en milieu argileux pour le project de stockage de déchets radioactifs en formation géologique. *Project Archimède argile, Rapport final*, EUR 17454 FR.

Heremans R., Barbreau A. & Bourke P. (1980) Thermal aspects associated with the disposal of waste in deep geological formations. Pp. 468–487 in: *Radioactive Waste Management and Disposal* (R. Simon & S. Orlowski, editors). Proceedings of the First European Community Conference, Luxembourg, May 20–23, Harwood Academic Publishers, Newark, New Jersey, USA.

Honty M. (2010) CEC of the Boom Clay – a review. *External Report of the Belgian Nuclear Research Centre*, Mol, Belgium: SCK·CEN–ER–134, 26 p.

Ignasiak T.M., Zhang Q., Kratochvil B., Maitra C., Montgomery D.S. & Strausz O.P. (1985) Chemical and Mineral Characterization of the Bitumen-Free Athabasca Oil Sands Related to the Bitumen Concentration in the Sand Tailings from Syncrude Batch Extraction Test. *AOSTRA Journal of Research*, **2**, 21–35.

Jackson M.L. (1975) *Soil Chemical Analysis – Advanced Course, 2nd edition*. Published by the author, Madison, Wisconsin, USA, 895 pp.

Kleeberg R. (2005) Results of the second Reynolds Cup contest in quantitative mineral analysis. *International Union of Crystallography. Commission on Powder Diffraction Newsletter*, **30**, 22–24.

Laenen B. (1997) The geochemical signature of relative sea-level cycles recognized in the Boom Clay. PhD Thesis, K.U. Leuven, Belgium.

Laenen B. (1998) The geochemical signature of relative sea-level cycles recognised in the Boom Clay. *University Press Leuven, Aardkundige Mededelingen*, **9**, 61–82.

Laenen B. & De Craen M. (2004) Eogenetic siderite as an indicator for fluctuations in sedimentation rate in the Oligocene Boom Clay Formation (Belgium). *Sedimentary Geology*, **163**, 165–174.

Lindgreen H., Drits V.A., Sakharov B.A., Salyn A.L., Wrang P. & Dainyak L.G. (2000) Illite-smectite structural changes during metamorphism in black Cambrian Alum shales from the Baltic area. *American Mineralogist*, **85**, 1223–1238.

Lindgreen H., Drits V.A., Sakharov B.A., Jakobsen H.J., Salyn A.L., Dainyak L.G. & Kroyer H. (2002) The structure and diagenetic transformation of illite-smectite and chlorite-smectite from North Sea Cretaceous-Tertiary chalk. *Clay Minerals*, **37**, 429–450.

McCarty D.K., Theologou P.N., Fischer T.B., Derkowski A., Stokes M.R., & Ollila A. (2015) Mineral-chemistry quantification and petrophysical calibration for multi-mineral evaluations: The *BestrockT* Approach. *AAPG Bulletin*. (Submitted).

Meier L. & Kahr G. (1999) Determination of cation exchange capacity (CEC) of clay minerals using the complexes of copper(II) ion with triethylenetetramine and tetraethylenepentamine. *Clays and Clay Minerals*, **27**, 417–422.

Merceron T., Mossmann J.R., Neerdael B., De Cannière P., Beaucaire C., Daumas S., Bianchi A. & Christen, R. (1993) Acquisition et régulation de la chimie des eaux en milieu argileux. *Projet Archimede-Argile, Rapport d'avancement semestriel no. 3* – ANDRA, 696 RP BRG 93–001.

Moore D.M. & Reynolds R.C., Jr. (1997) *X-ray Diffraction and the Identification and Analysis of Clay Minerals*. Oxford University Press, Oxford-New York, 378 pp.

Omotoso O., McCarty D.K., Hillier S. & Kleeberg R. (2006) Some successful approaches to quantitative mineral analysis as revealed by the 3rd Reynolds Cup Contest. *Clays and Clay Minerals*, **54**, 748–760.

ONDRAF/NIRAS (2013) *ONDRAF/NIRAS Research, Development and Demonstration Plan for the geological disposal of high-level and/or long-lived radioactive waste including irradiated fuel if considered as waste. State-of-the-art report as of December 2012*. NIROND–TR 2013–12.

Renngarten N.V., Rateev M.A., Shutov V.D. & Drits V.A. (1978) Lithology and clay mineralogy of sediments from site 337, DSDP Leg 38. *Deep Sea Drilling Project Report and Publications, DSDP* Supplement to Volumes **38**–**41**.

Reynolds R.C. (1986) The Lorentz-Polarization factor and preferred orientation in oriented clay aggregates. *Clays and Clay Minerals*, **34**, 359–367.

Sakharov B.A., Lindgreen H., Salyn A.L. & Drits V.A. (1999) Determination of illite-smectite structures using multispecimen X-ray diffraction profile fitting. *Clays and Clay Minerals*, **47**, 555–566.

Sakharov B.A, Dubinska E., Bylina P., Kozubowsk J.A., Kapron G. & Frontczak-Baniewicz M. (2004) Serpentine-smectite interstratified minerals from Lower Silesia (SW Poland). *Clays and Clay Minerals*, **52**, 55–65.

Środoń J. (2009) Quantification of illite and smectite and their layer charges in sandstones and shales from shallow burial depth. *Clay Minerals*, **44**, 421–434.

Środoń J., Drits V.A., McCarty D.K., Hsieh J.C.C. & Eberl D.D. (2001) Quantitative X-ray diffraction analysis of clay-bearing rocks from random preparations. *Clays and Clay Minerals*, **49**, 514–528.

Środoń J. & McCarty D.K. (2008) Surface area and layer charge of smectite from CEC and EGME/H_2O-retention measurements. *Clays and Clay Minerals*, **56**, 155–174.

Środoń J. & Kawiak T. (2012) Mineral compositional trends and their correlations with petrophysical and well-logging parameters revealed by Quanta + Bestmin analysis: Miocene of the Carpathian Foredeep, Poland. *Clays and Clay Minerals*, **60**, 63–75.

Thorez J. (1976a) *Rapport d' analyse minéralogique: contenu qualitative et semi-quantitatif en minéraux argileux dans l'argile de Boom, au site de Mol* (C.E.N.). 325/07/030 MiUL. 19 pp. 10 Fig. (rapport pour SCK–CEN).

Thorez J. (1976) *Practical Identification of Clay Minerals. A Handbook for Students and Teachers in Clay Mineralogy* (G. Lelotte, editor). Dison, Belgium, 90 pp.

Ufer K., Kleeberg R., Bergmann J. & Dohrmann R. (2012) Rietveld refinement of disordered illite-

smectite mixed-layered structures by a recursive algorithm. II: Powder-pattern refinement and quantitative phase analysis. *Clays and Clay Minerals*, **60**, 535–552.

Vandenberghe N. (1978) Sedimentology of the Boom Clay (Rupelian) in Belgium. *Memoirs of the "Koninklijke Academie voor Wetenschappen, Letteren en Schone Kunsten van Belgie", Klasse der Wetenschappen*, **XL**, Nr 147, 137 pp.

Vandenberghe N. & Mertens J. (2013) Differentiating between tectonic and eustatic signals in the Rupelian Boom Clay cycles (Oligocene, Southern North Sea Basin). *Newsletters on Stratigraphy*, **46/3**, 319–337.

Vandenberghe N. & Thorez J. (1985) XRD-onderzoek van de 14 Å componenten in de kleimineralenfraktie van de Boomse klei in de boring te Mol 31W–237. Geological Survey of Belgium, unpublished report, 10 pp..

Vandenberghe N., Hager H., van den Bosch M., Verstraelen A., Leroi S., Steurbaut E., Prüfert J., & Laga P. (2001) Stratigraphical correlation by calibrated well logs in the Rupel Group between North Belgium, the Lower-Rhine area in Germany and Southern Limburg and the Achterhoek in The Netherlands. *Aardkundige Mededelingen*, University Press Leuven, **11**, 69–84.

Vandenberghe N., Herman J. & Steurbaut E. (2002) Detailed Analysis of the Rupelian Ru-1 Transgressive Surface in the Type Area (Belgium). Pp. 67–83 in: *Northern European Cenozoic Stratigraphy* (K. Gürs, editor). Proceedings 8th Biannual Meeting RCNNS/RCNPS. Flintbek, Landesamt für Natur und Umwelt des Landes Schleswig-Holstein, Germany.

Vandenberghe N., De Craen M. & Wouters L. (2014) The Boom Clay geology. From sedimentation to present-day occurrence. A review. *Royal Belgian Institute of Natural Sciences, Memoirs of the Geological Survey of Belgium*, **60**, 76 pp.

Varentsov I.M., Sakharov B.A. & Eliseeva T.G. (1983) Clay components of post middle Jurassic sediments of the southwest Atlantic, Deep Sea Drilling Project, Leg 71: depositional history and authigenic transformations. *Deep Sea Drilling Project Report and Publications. DSDP Volume* **71**

Volckaert G., Neerdael B., Manfroy P. & Lalieux Ph. (1994) *Characteristics of argillaceous rocks. A catalogue of the characteristics of argillaceous rocks studied with respect to radioactive waste disposal issues: Belgium, Canada, France, Germany, Italy, Japan, Spain, Switzerland, United Kingdom and United States*. Revision number 1.2–30/06/1994.

Welkenhuysen K., Vancampenhout P. & De Ceukelaire M. (2012) Quasi-3D model van de Formatie van Maldegem, De Groep van Tongeren en de Groep van de Rupel. *Geological Survey of Belgium Professional Paper 2012/1*, **311**, 46 pp.

Wouters L., Herron M., Abeels V., Hagood M. & Strobet J. (1999) Innovative application of dual range Fourier transform infrared spectroscopy to analysis of Boom Clay mineralogy. *University Press Leuven, Aardkundige Mededelingen*, **9**, 159–168.

Zeelmaekers E. (2011) *Computerized qualitative and quantitative clay mineralogy. Introduction and application to known geological cases*. PhD Thesis, K.U. Leuven, Belgium, 397 pp. (https://lirias.kuleuven.be/handle/123456789/306162).

https://doi.org/10.1180/claymin.2015.050.2.08 Published online by Cambridge University Press